Available online at www.sciencedirect.com

SCIENCE DIRECT®

polymer

Polymer 46 (2005) 3528–3534

www.elsevier.com/locate/polymer

Dynamic mechanical properties of whisker/PA66 composites at high strain rates

Xiangyang Hao[a], Guosheng Gai[a,*], Fangyun Lu[b], Xijin Zhao[b], Yihe Zhang[c], Jiping Liu[d], Yufen Yang[a], Dayong Gui[d], Ce-wen Nan[a]

[a]*Department of Materials Science and Engineering, Tsinghua University, Beijing 100084, People's Republic of China*
[b]*Institute of Technical Physics, National University of Defense Technology, Changsha 410073, People's Republic of China*
[c]*Technical Institute of Physics and Chemistry, Chinese Academy of Sciences, Beijing 100080, People's Republic of China*
[d]*School of Materials Science and Engineering, Beijing Institute of Technology, Beijing 100081, People's Republic of China*

Received 1 November 2004; received in revised form 5 January 2005; accepted 3 February 2005
Available online 16 March 2005

Abstract

PA66 reinforced with potassium titanate whisker (TKW) treated with silane coupling agent were prepared using a twin-screw extruder. The quasi-static and dynamic mechanical properties were investigated. Addition of 40 wt % TKW to PA66 improves all the investigated properties. The high-speed dynamic tests with TKW/PA66 were carried on split Hopkinson pressure bar (SHPB). The loading pulses in SHPB experiments were precisely controlled to ensure that the composite specimens deformed at a nearly constant strain rate under dynamically equilibrated stress during dynamic compression. The constitutive curves and equations at high strain rates have been obtained. TKW/PA66 composites show 20–100% increase on reference modulus and 20% increase on compression strength.

Keywords: Potassium titanate whisker (TKW); Composite; Split Hopkinson pressure bar (SHPB)

1. Introduction

Whiskers are short and fiber-shaped single crystals with high perfection and large length–radius-ratio. Owing to their small diameters, whiskers are nearly free of internal defects, thereby yielding a strength close to the maximum theoretical value predicted by the theory of elasticity. Thus whiskers are considered to be an attractive alternative to short glass or carbon fibers for reinforcing thermoplastics. Various inorganic whiskers, such as calcium carbonate whisker, aluminium oxide whisker and TKW were prepared and employed in manufacturing of composites with different thermoplastic matrices. Previous researchers have demonstrated that whiskers have much higher specific strength than short glass or carbon fibers [1–8]. They can reinforce thermoplastics more effectively and the whisker/polymer composites are very often of mechanical properties superior to both short-glass or carbon fiber composites, for example, Tjong and Meng [1–3] reported that the quasi-static tensile properties of PA6 can be improved significantly by addition of TKW. Moreover, it is more cost effective to use TKW to reinforce polymers.

It is well known that many polymeric composites have been characterized under quasi-static loading conditions. However, the mechanical properties of polymeric composites under dynamic loading conditions are much less understood, partially due to the associated experimental difficulties at high strain rates, to our best knowledge the dynamic mechanical behavior of TKW/PA66 has not been observed yet.

Many of the applications for composite materials are impact related, reliable material models that accurately describe the responses of such composites under not only quasi-static but also dynamic loading conditions are necessary for structural design and optimization purposes. Furthermore, all materials need reliable experimental data in order to describe the constitutive behavior, to determine

* Corresponding author. Tel.: +86 10 62781144; fax: +86 10 62791258.
E-mail address: gaigs@tsinghua.edu.cn (G. Gai).

0032-3861/$ - see front matter © 2005 Elsevier Ltd. All rights reserved.
doi:10.1016/j.polymer.2005.02.042

the material constants, and to examine the accuracy of the models over the ranges of their applications [9–20].

In the present study, we will modify whisker surface, then extrude with PA66 to prepare a group of TKW/PA66 composites with whisker content from 30 to 50 wt %, investigate their quasi-static and dynamic mechanical properties.

2. Experimental

2.1. Materials

The whiskers used in this study were TKW purchased from JinJian Composite Co., Shenyang, China. Their properties are listed in Table 1 [1]. The *g*-methacryloxy-propyltrimethoxy silane (KH-550) used as the coupling agent for TKW was received from Nanjing Shu Guang Chemical Co. Nanjing, China. PA66 (AKULON S-223E) was commercially available from DSM, Netherlands.

2.2. Treatment of whiskers

Surface treatments for fillers have been adopted to improve the interfacial interaction between fillers and polymeric matrix, thereby allowing a better shear stress transfer between the fillers and matrix. Therefore the surface of TKW was treated with silane coupling agent KH550 before blending according to our previous study. Dispersion quality of TKW in PA66 matrix and the degree of interfacial adhesion between PA66 and whisker are the key points of this composite. KH550 of 1.5 wt % of whisker was dissolved in ethanol aqueous solution (the weight ratio of ethanol to distilled water was fixed at 9:1) to form a solution in which KH550 was 50 wt %, and the pH of the solution was adjusted to 4–5 with acetic acid.

During processing, whisker is prone to be fractured due to its large length-to-diameter ratio. Surface treatment process is very important. Mixer with high speed is not suitable for the treatment. The higher the speed is, the more possible the whisker will be damaged. The longer the treatment time is, the more disastrous damage the whisker will receive. So shorter treating time is better to avoid destroying whisker. But shorter time is not beneficial to uniformly covering of whisker. To balance the damage and uniformly covering, mixer filled with 1 kg whiskers started at 2000 rpm for 1 min to eliminate agglomeration of whisker, and then treatment solution was sprayed slowly into a high-speed mixer filled with whisker to blend for 1 min. After dripping and stirring for 1 min, the treated whisker was moved into an oven and heated at 100 °C for 4 h to remove the solvent.

2.3. Sample preparation

PA66 was air-dried at 110 °C for 3 h to avoid moisture-induced degradation reactions. PA66 and 30, 35, 40, 45, and 50 wt % TKW were extruded, respectively, by an extruder with a screw speed of 122 rpm, and a feed rate of 11 rpm. The temperature profiles of the barrel were 195–205–215–235–245–250–265–265–260 °C from the hopper to the die. These extrudates were then palletized, dried and injected into standard samples for quasi-static mechanical testing. The specimens for dynamic mechanical tests at high strain rates were cylinders with 13.7 mm in diameter and 6 mm in length.

2.4. Quasi-static mechanical properties

Notched Charpy impact strength, flexural strength/modulus, tensile strength, and heat distortion temperature (HDT) were measured, respectively, according to Chinese National Standard GB1043-79, GB9341, and GB/T1040, GB1634-79, which refer to the corresponding ASTM. Ten specimens were tested for getting impact strength for each composite, five specimens were tested for obtaining bending and tensile strength.

2.5. Scanning electron microscopy (SEM)

The impact test specimens of TKW/PA66 composite were examined in a scanning electron microscope (SEM Hitachi 4500), after the fractured surfaces were coated with a thin layer of gold (see Fig. 1).

2.6. Dynamic mechanical properties at high strain rates

The dynamic compressive tests were conducted on split Hopkinson bars (SHPB) in Institute of Technical Physics, National University of Defense Technology. A schematic of SHPB facility is shown in Fig. 2.

SHPB was composed of striker, incident bar, transmission bar, and the specimen was sandwiched between incident bar and transmission bar, see Fig. 2. Along the axis, the striker impacted the incident bar at a certain speed, which induced compressive stress waves propagating in the bars.

The lengths of the 20 mm-diameter striker, incident, and

Table 1
Properties of TKW

Material	Density ($\times 10^3$ kg/m^3)	Length (mm)	Diameter (μm)	Tensile strength (GPa)	Tensile modulus (GPa)	Moh hardness
$K_2Ti_6O_{13}$	3.3	10–40	0.5–1.0	7	280	4

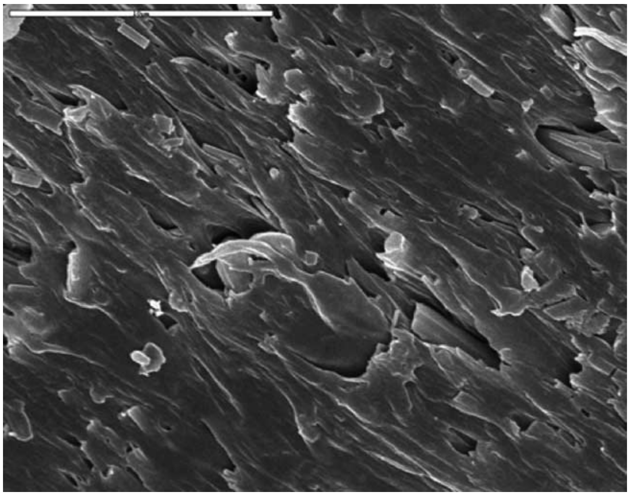

Fig. 1. SEM micrograph of 35%TKW/PA66 composite.

transmission bars were 150, 1980 and 1000 mm, respectively. In our work, the bars were made of 40Cr-steel, of which density and Young's modulus were 7.85×10^3 kg/m^3 and 210 GPa, respectively.

KD205-1A dynamic strain-meter and Lecroy9370 (1GSPS) digital storage oscilloscope were used for signal record during the testing. The strains were recorded by gauges mounted on the surfaces of the bars. Copper disks were used at impact end of the incident bar to precisely control the profile of the loading (incident) pulse in order that the specimen deformed at a nearly constant strain rate under dynamically equilibrated stress.

Impact speed of the striker was recorded by an IR optic-electronic probe speedometer. The speed can be expressed in the form

$$u = \frac{\Delta s}{\Delta t} \tag{1}$$

where Δs represents the distance between IR speedometer probes, Δt is the time taken by the strike to pass the distance. The speed signal was recorded by KD205-2B IR speedometer and Tek2440 400 Hz digital store oscilloscope.

3. Results and discussion

3.1. Outcomes of quasi-static mechanical properties

The outcomes of the quasi-static mechanical properties of the TKW/PA66 composites are shown in Table 2. Compared with G0, there are some improvement of properties in case of the composite G2 and G3. For G3, the tensile strength is increased by 17.1%, flexural strength is increased by 17.7%, flexural modulus is increased by 109.4%, HDT is increased by 114.6%. Addition of TKW leads almost no decrease in impact strength. For composite G2, Notched Charpy impact strength is increased by 23.3%. The discrepancy in experimental results can be attributed to the presence of aggregates or voids, etc.

A small amount of coupling agent can improve the dispersion quality of TKW and interfacial adhesion degree between TKW and matrix; so when under impact, the force was transferred to the whiskers through interface, and the whiskers become the receptor of the foreign force. More TKW means more impact receptor. But if the content of whiskers exceed the threshold, the toughening efficiency decreases. On one hand, too many whiskers will rub against each other seriously when they are extruded with matrix, length–radius-ratio will decrease. On the other hand, it is difficult to disperse so many TKW well, which also leads to the decrease of impact strength. Experiment result shows 35–40% TKWs is best. As tensile strength and flexural modulus were considered, we chose G3 for SHPB test.

3.2. The microstructures of composites and fracture mechanisms

The main fracture mechanism of TKW/PA66 is debonding (dewetting) of whisker and yielding of matrix. Fig. 1 shows that TKWs are detached from the polymer matrix and the matrix exhibits extensive plastic deformation. This is consistent with the proposed mechanism that debonding of fillers from the matrix induce shear yielding of the matrix, and hence give rise to extra dissipation of impact energy.

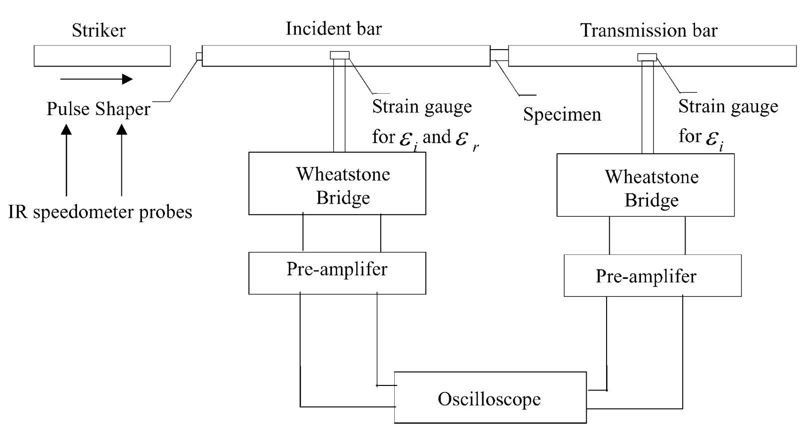

Fig. 2. Schematic diagram of the pulse-shaped SHPB setup.

Table 2
Quasi-static mechanical properties of TKW/PA66 composites

	G0 (VirginPA)	G1 (30% TKW)	G2 (35% TKW)	G3 (40% TKW)	G4 (45% TKW)	G5 (50% TKW)
Notched Charpy impact strength[a] ($J\ m^{-1}$)	7.3	7	9	7.1	7.8	7.3
Tensile strength[a] (MPa)	85.4	98.3	98.6	100	89.3	90.7
Elongation of break[b] (%)	40	33	30	36	25	25
Flexural strength[a] (MPa)	119.5	128.1	140.2	140.7	132.5	124.2
Flexural modulus[b] (MPa)	2170	3375	3683	4545	3923	4868
HDT[c] (°C)	98.8	205.8	196.2	212	194.3	208.4

[a] Relative probable error 5%.
[b] Relative probable error 10%.
[c] Relative probable error 2%.

When content of TKW exceed optimum value, there is less matrix shear yielding, the matrix ligament thickness is very small, and stress whitening only occurs on the fracture surface; the surface-to-surface interwisker distance (matrix ligament thickness) and the effective matrix cross-section become very small, and the local constrain in the polymer matrix near TKW increases. As a result, cracks will propagate faster and the matrix beneath the fracture surface will be prohibited from deforming plastically, thereby resulting in a decrease in the impact strength. Shear yielding of the polymer matrix induced by debonding at the interface between TKW and PA is shown to be fracture mechanism [21,22].

3.3. The experimental waveform

Assuming that there is only elastic deformation in the incident bar, and stress waves propagate along the bars one-dimensionally. Upon the stress waves arrive at the specimen, one part of the waves will be reflected back to the incident bar, one part of the waves will act on the specimen and pass through the specimen into the transmission bar. When the width of the stress waves are much longer than the duration of the waves passing through the specimen, we can assume that the specimen is in a condition of uniform deformation and stress equilibrium during the majority of process of the loading. Then we have $P_1 = P_2$, P_1 represent the force acting on the front face of the specimen, P_2 represents that on the back face. When the incident bar and the transmission bar are made of the same material, with the same cross-section area, we can deduce an equation as $\varepsilon_t = \varepsilon_i + \varepsilon_r$. Where ε_i, ε_r, ε_t represent real-time strains caused by incident, reflected, and transmitted waves in the bar, respectively. These strains can be recorded by gauges mounted on the surfaces of the bars [10].

Fig. 3 shows a typical waveform record. The solid line represents the incident record ε_i and reflected record ε_r. Dotted line represents transmitted record ε_t. A special phenomenon is that, there is a large opposite unloading wave late in the reflected wave. This is the phenomenon of elastic hysteresis effect, which may be caused by viscoelastic response of this kind of polymer.

3.4. Data processing

$\varepsilon_i(t)$, $\varepsilon_r(t)$ and $\varepsilon_t(t)$ can be obtained by processing incident, reflected and transmitted signals, the subscripts (i, r, and t) denote the corresponding quantities of incident, reflected, and transmitted waves, respectively. Engineering stress and strain can be deduced from Eqs. (2) and (3) [10–17].

$$\sigma(t) = \frac{A_0}{A_s} E \varepsilon_t(t) \tag{2}$$

$$\varepsilon(t) = \int -\frac{2C_0}{L} \varepsilon_r(t) \mathrm{d}t \tag{3}$$

where E is the young's modulus of the bar, A_0 is the cross-sectional area of the bar, C_0 is the speed of the elastic wave in the bar, L is the length of the specimen, A_s is the cross-sectional area of the specimen.

The constitutive relation (stress–strain curve) of the material can be deduced from Eqs. (2) and (3).

The validity of data processing can be verified by force equilibrium at two ends of specimen.

True stress–strain can be obtained from the engineering

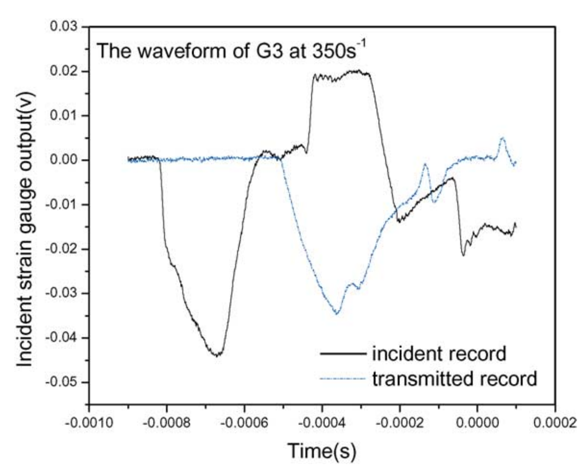

Fig. 3. Typical oscilloscope recorded signals of a SHPB experiment on specimen.

stress–strain by following formulations:

$$\begin{cases} \sigma_t(t) = (1-\varepsilon(t))\sigma(t) \\ \varepsilon_t(t) = -\ln(1-\varepsilon(t)) \end{cases} \quad (4)$$

where $\sigma_t(t)$, $\varepsilon_t(t)$ represent true stress and true strain, respectively, $\sigma(t)$ and $\varepsilon(t)$ represent engineering stress and strain, respectively. All stress–strain curves listed in the thesis are true stress and true strain.

3.5. Constant strain rate loading

Traditionally, SHPB test is loaded by direct impact on striker, the incident pulses are in square form. From Eq. (3), reflected wave represents the state of strain rate, a square reflected wave form means a constant strain rate. Affected by transmission waveform, (i.e. the response of material), reflected waves are difficult to be ensured in constant strain rate. The technique of incident pulse shaping is to mount a smaller diameter pulse shaper ahead of impact end of the incident bar. During the loading process, the striker impacts pulse shaper firstly, the plastic deformation of pulse shaper changes the loading wave-form in the incident bar. Incident signal can be adjusted by changing the material and size of the pulse shaper. The original goal of pulse shaper is to filter out high-frequency components of the loading waves caused by directly hitting, which can reduce wave dispersion during a long distance propagation. Pulse shaper is helpful to get higher quality signal [18–20].

Through theoretic prediction and trial experiment, we select copper disks with diameter of 6.5–14.5 mm as pulse shaper. In Fig. 3, the solid line represents an incident and the response to it, the dotted line represents the transmitted record. In the solid line, the valley means an incident pulse, the high plateau means the reflected pulse (the response). The nearly flat plateau indicates that the specimen deformed at a nearly constant strain rate. Fig. 4 shows typical curves of the strains rate and strain at constant strain rate. In Fig. 4, loading 20 μs later and before unloading, the waveform of stain rate looks flat.

The corresponding strain shows a linear increase in the majority of deformation process after the strain is more than 0.01, which is the valid range of the test. The strain in (Fig. 4(b)) is the integral result of strain rate to time (Fig. 4(a)). 0.01 is safe for all kinds of strain rate in Fig. 4.

3.6. Dynamic compression stress–strain curves of virgin PA66 (G0)

Fig. 5 shows stress–strain curves of G0 at strain rates of 400, 1000 and 1500 s^{-1}. Three curves correspond to polynomial fitted curve of experimental data at three strain rates. The constants of fitted curve are listed in Table 3. At the strain rate of 400 s^{-1}, G0 shows a typical viscoelastic response of polymer: delayed deformation and stress relaxation. Stress at the failure point is about 110 MPa. At the strain rate of 1000 s^{-1}, the stress–strain curve shows a point of inflection like a kind of yield point, then takes on strain hardening. At the strain rate of 1500 s^{-1}, after the point of inflection, the stress–strain curve shows a response of ideal plasticity. We refer the value of stress at the inflection point as yield strength of the material. The curves show that the strength increases with strain rate. The strength is about 110 MPa at the strain rate of 1000 s^{-1}, and 130 MPa at 1500 s^{-1}. The strains at the point of inflection are quite different from each other for two strain rates are concerned. This shows that stiffness of the material changes evidently with strain rate. Dynamic modulus is not conclusive from the testing curves, because unavoidable effects of wave propagation at the early stage of the experiments. As a reference, we still define the stiffness of material by using the slope of stress–strain curve, we call it reference modulus. At the strain rate of 1500 s^{-1}, the reference modulus of PA66 is 25% higher than that at the strain rate of 400 s^{-1}. The difference of the stiffness between the strain rates of 400 and 1000 s^{-1} is obvious as well except the effects of wave propagation at the early stage of the experiments.

There is no definite relation between material properties in higher strain-rate and lower strain-rate, or weakening, or hardening. That is so-called strain-rate effect of material behaviors. PA66 shows hardening of strain rate in the

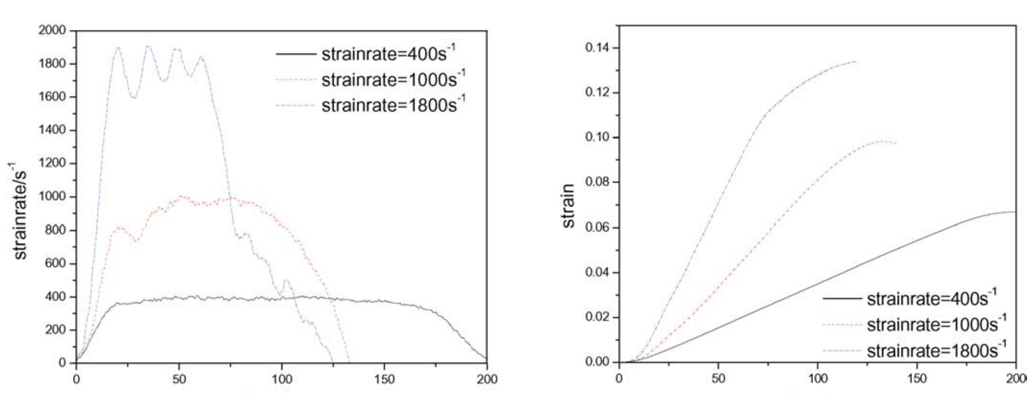

Fig. 4. Curves of strain rates and strains at constant strain rate.

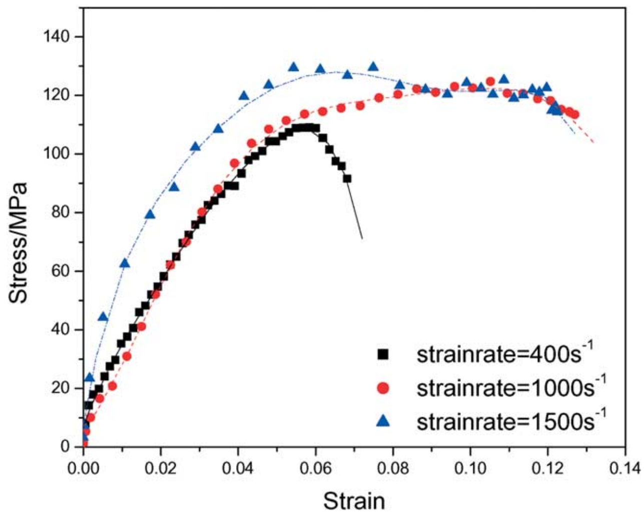

Fig. 5. Stress–strain curves of G0 at three strain rates.

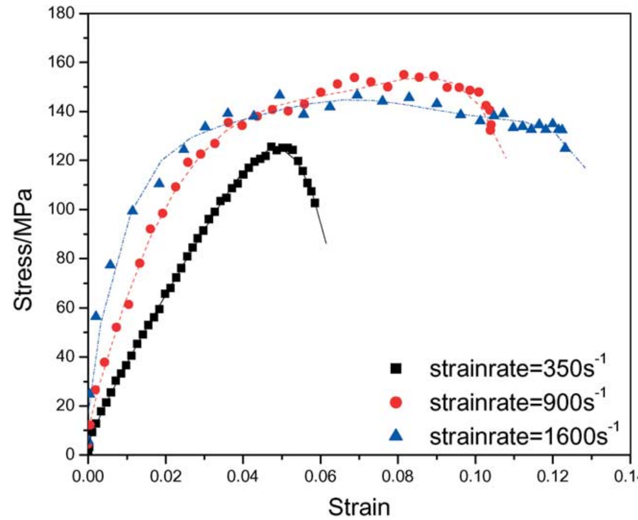

Fig. 6. Stress–strain curves of G3 at three strain rates.

experiment. This may be caused by the relaxation of polyamide chain. At lower rate, the motion of polyamide chain keeps up with the strain rate, and responds more fully, which causes larger deformation. At higher rate, the motion of polyamide can not keep up with the strain rate, and responds less fully, which causes smaller deformation at the same strain rate.

3.7. Dynamic compression stress–strain curves of composite 40 wt %/PA66 (G3)

The studies clearly indicate an increase in strength value as the rate of deformation increases. Fig. 6 shows true stress–strain curves of G3 at strain rate of 350, 900, and 1600 s^{-1}. For G3, strain rate effects mainly show on an increase of deformation stiffness. The reference modulus at higher strain rate is twice of that at lower strain rate. The influence of strain rate on strength is not evident and the value of strength is about 125 MPa. Although the stress–strain curves of G3 take on similar form as G0, the strengths are different from G0 obviously, especially the stiffness. At the same strain rate, compared with virgin PA66, 40 wt %/PA66 shows a great increase on mechanical properties, especially the deformation stiffness. The biggest increment on modulus is 100%. The biggest increment on strength is about 20%.

3.8. Comparison of dynamic compressive constitutive curves of G0 and G3

In dynamic experiments at high strain rates, it is very different to make strain rates in two tests just totally the same. Strain rates for G0 were 400, 1000, 1500 s^{-1}, respectively. Strain rates for G3 were 350, 900, 1600 s^{-1}, respectively. Strain rates of 400, 350 s^{-1} are in the same region which can be compared each other, so are 1000, 900 s^{-1}; and 1500, 1600 s^{-1} in SHPB experiment.

At the similar strain rate, compared with G0, the properties of G3 increase evidently. At the rate of 400 and 1000 s^{-1}, the compressive strengths of G3 increase 20%. At three strain rates, the modulus increases more than 20%. At different strain rates, the increments are different and the maximum increment is 100%.

At the similar strain rate, all stress–strain curves of G0 and G3 show similar features: at strain rate of 400 s^{-1}, G0 and G3 show typical viscoelastic responses of polymers: nonlinear deformation and delayed deformation after material failure. At the rate of 1000 s^{-1}, the stress–strain curves show a point of reflection just like yield point, then the materials take on a constitutive response with strain hardening. At the rate of 1500 s^{-1}, behind the yield point of reflection, the stress–strain curves show a constitutive

Table 3
Constants of constitutive polynomial

	Strain rate (s^{-1})	A0	A1	A2	A3	A4	A5	A6
G0	400	7.62	3.53×10^{-3}	-1.17×10^{-5}	5.28×10^{-6}	-1.35×10^{-8}	1.73×10^{-9}	-9.13×10^{-9}
	1000	5.60	1.60×10^{-3}	8.95×10^{-4}	-2.89×10^{-6}	3.33×10^{-7}	-1.70×10^{-8}	3.10×10^{-8}
	1500	10.74	6.81×10^{-3}	-2.37×10^{-5}	5.61×10^{-6}	-7.66×10^{-7}	5.23×10^{-8}	-1.38×10^{-9}
G3	350	4.91	3.72×10^{-3}	-5.58×10^{-4}	1.02×10^{-6}	6.27×10^{-6}	-3.0×10^{-8}	0
	900	11.47	6.27×10^{-3}	-9.83×10^{-4}	4.71×10^{-5}	-6.38×10^{-5}	4.97×10^{-7}	-4.15×10^{-8}
	1600	23.57	1.06×10^{-4}	-4.4×10^{-5}	9.81×10^{-6}	-1.18×10^{-8}	7.14×10^{-8}	-1.71×10^{-9}

response of ideal plasticity. This shows that TKW/PA66 has a trend of toughness enhancing at high strain rate.

The character of plastic-deformation can be seen from stress–strain curve, especially at high strain rate, but there is little obvious residual deformation from recovered specimens. This must be a result of visoelastic recovery of the material.

3.9. The constants of stress–strain equation

The constants of Eq. (5) are obtained by fitting the experimental data at different strain rates, and then the constitutive curve equation in form of polynomial has been obtained. Table 3 shows the polynomial constants of virgin PA 66 and TKW/PA66 at different strain rates.

The polynomial expression of stress–strain relation is in form of

$$\sigma = a_0 + a_1\varepsilon + a_2\varepsilon^2 + a_3\varepsilon^3 + a_4\varepsilon^4 + a_5\varepsilon^5 + a_6\varepsilon^6 \qquad (5)$$

the unit of σ is MPa.

Physical meaningful constitutive relations of materials are an advanced research field in this area.

In this study, whisker is extruded with PA66 in the first feeding hopper, so the length–radius-ratio decreased. If whisker is put into the second feeding hopper, while PA66 is kept still in the first hopper, the distance that the whisker removes will be cut, so alleviate the hurt of whisker. This will improve the properties of TKW/PA66 composite greatly. This requires that the speed of the first feeding hopper, the second feeding hopper, and extrude should be controlled cautiously. In following papers, we will discuss the technological conditions involved.

4. Conclusion

The incorporation of whisker into PA66 leads to increase in stiffness, strength, fracture toughness and heat-resistance property. A modified SHPB technique was conducted on dynamic compressive experiments to ensure that stress and strain data were obtained from a specimen under homogeneous deformation and dynamic stress equilibrium:

(1) At the rate of $400\ \mathrm{s}^{-1}$, virgin PA66 and TKW/PA66 show a typical viscoelastic constitutive behavior of polymer. At the rate of $1000\ \mathrm{s}^{-1}$, stress–strain curve shows a yield reflection point then strain hardening. At the rate of $1500\ \mathrm{s}^{-1}$, behind the point of reflection, stress–strain curves show an ideal plastic constitutive response. The strains at the point of reflection are quite different, which depend on material and the strain rate. This shows the stiffness of materials is quite different. In the experimental range, virgin PA66 and KTW/PA66 show strain rate related response. The strain rate effects mainly show on the deformation stiffness.

(2) At the same strain rate, compared with virgin PA66, the properties of TKW/PA66 have been improved evidently. For example, the reference modulus are increased by 20–100% the maximum increment on compression strength is 20%.

Acknowledgements

The authors thank the Natural Science Foundation of P. R. China (Contract no. 50474003).

References

[1] Tjong SC, Meng YZ. Polymer 1999;40:1109.
[2] Tjong SC, Mend YZ. Polymer 1998;39:5461.
[3] Tjong SC, Meng YZ. Polymer 1999;40:7275.
[4] Lü JZ, Lu XH. J Appl Polym Sci 2001;82:368.
[5] Ou YC, Yang F, Chen J. J Appl Polym Sci 1997;64:2317.
[6] Tjong SC, Meng YZ. J Appl Polym Sci 1999;72:501.
[7] Jiang W, Tjong SC. Polym Degrad Stab 1999;66:241.
[8] Yu DM, Wu JS, Zhou LM, et al. Compos Sci Technol 2000;60:499.
[9] Park SW, Zhou M. J Compos Mater 2000;34:883.
[10] Gama BA, Gillespie JW, Mahfuz H, et al. J Compos Mater 2001;35:1204.
[11] Casem DT, Fourney WL, Chang P. Exp Mech 2003;43:423.
[12] Song B, Chen W, Weerasooriya T. J Compos Mater 2003;37:1725.
[13] Chen W, Song B, Frew DJ, et al. Exp Mech 2003;43:21.
[14] Frew DJ, Forrestal MJ, Chen W. Exp Mech 2002;42:95.
[15] Vaidya UK, Hosur MV. J Thermoplast Compos Mater 2003;16:78.
[16] Cheng ZQ, Crandall JR, Pilkey WD. Shock Vibrat 1998;5:308.
[17] Chen W, Lu F, Winfree N. Exp Mech 2002;(42):67.
[18] Hosur MV, Abraham A, Jeelani S. J Compos Mater 2001;35:1117.
[19] Li ZH, Bi XP, Lambros J. Exp Mech 2002;42:419.
[20] Haque A, Hossain MK. J Compos Mater 2003;37:631.
[21] Liu ZH, Kwok KW, Lib RKY, Choy CL. Polymer 2002;43:2504.
[22] Osman MA, Atallah A, Suter UW. Polymer 2004;45:1180.